

# A Review Study On Laser Shock Forming To A Newly Proposed Technique On Micro-Forming Using Metallic Foils.

Jamal-Deen Kukurah<sup>1</sup>, James Kwasi Quaisie<sup>2</sup>, Enock Asuako Larson<sup>3</sup>, Vitus Mwinteribo Tabie<sup>4</sup>, Anthony Akayeti<sup>1</sup>, Joseph Sekyi-Ansah<sup>5</sup>, Abdul-Hamid Mohammed<sup>2</sup>, Philip Yamba<sup>1</sup>, Bismark Addai<sup>6</sup>.

<sup>1</sup>Faculty of Engineering (Mechanical Engineering Department, Tamale Technical University, Tamale, Ghana.

<sup>2</sup>Faculty of Engineering (Welding & Fabrication Department, Tamale Technical University, Tamale, Ghana

<sup>3</sup>Mechanical and Industrial Eng. Department, Faculty of Engineering, University for Development Studies, GHANA

<sup>4</sup>Faculty of Engineering (Mechanical Engineering Dept.), Hila Liman Technical University, Wa, 00233, Ghana

<sup>5</sup>Mechanical Engineering Department, Takoradi Technical University, Takoradi, Ghana

<sup>6</sup>Materials Engineering Department, Sunyani Technical University, Sunyani, Ghana

## Abstract

Laser Shock Forming (LSF) is a non-warm sheet metal forming process, utilizing the shock wave persuaded by laser radioactivity to change the curvature of the objective, for example, precisely bending, shaping, precision-align, altering, and additionally fixing designing parts. Because of its blend of uncommon manufacturing advantages, including non-warm, no hard tooling, high procedure adaptability and controllability, and peening impact for upgraded material sturdiness, LSMF has been utilized for extensive manufacturing applications in the microelectromechanical systems, automotive, biomedical devices, aerospace, microelectronics and shipbuilding. As a cutting-edge innovation, progressing examinations are being conducted to advance the adequacy of LSMF. This study aims to review the innovative work status of LSF. The LSF procedure configuration, forming mechanisms, and exploratory and theoretical examinations of the materials are deliberated. The disfigurement practices as influenced by laser preparing parameters, including laser intensity, material thickness, die diameter, and several scanning tracks, on different materials are reviewed. Furthermore, the ongoing advances in femtosecond LSF and warmth helped LSF be studied. Cavitation water jet impact on microforming process as a new technology is to be introduced.

**Keywords:** Laser shock forming, micro forming, forming mechanisms, deep drawing, cavitation water jet.

Date of Submission: 08-05-2024

Date of acceptance: 20-05-2024

## I. Introduction

Laser technology is one of the procedures for the manufacturing of micro parts. Up until now, it has been utilized broadly in micro forming, micro cutting, micro welding, material testimony and surface designing because of the confined laser beam control, process adaptability, and dependability [1, 2]. With the trend of miniaturization and integration becoming increasingly prominent, the application of parts with microfeatures is becoming more widespread in market areas such as telecommunication devices, medical devices, automotive industry, consumer electronics, etc. With the pattern of miniaturization and integration ending up progressively prominent, the utilization of parts with micro highlights is winding up increasingly across the board in market regions, for example, medicinal devices, consumer electronics, the automotive industry, media transmission devices, and so on. In the meantime, this has incredibly advanced the improvement of micromanufacturing technologies [3, 4]. Cold plastic bending is a kind of close net-shape forming innovation that has started numerous scientists' advantages for its potential application in the manufacture of micro parts [5, 6]. Among them, the micro-forming of foils is turning into a focal point of present research [7]. The micro forming of foils

incorporates micro bulging, micro drawing, micro bending, and so forth [3, 8, 9]. Among the microfabrication processes, micro metal forming is the most financially savvy procedure to create micro metallic parts with high accuracy in large-scale manufacturing [10, 11], with a little space prerequisite, and low consumption of energy [4, 8, 12, 13]. The metal forming innovation and knowledge on the macroscale have grown very much, yet they cannot be directly applied to microforming by just downsizing the components of tooling due to the alleged size impacts [14, 15]. The laser shock forming procedure is another procedure dependent on laser-induced shock waves [16-18]. As opposed to conventional laser forming of metal sheets, where warm instruments cause the bending of the sheets, the shock procedure depends on a non-warm forming procedure. The laser-induced shock wave can be utilized, on a fundamental level, for all metal sheet forming procedures as long as the parts are inside mesoscopic or micro size extents [19]. As of late, the genuine large-scale manufacturing fabricating procedures and micro and meso-forming of medical and electronic parts are drawing attention from both researchers and manufacturers in different fields. Though in downsizing the item measure, different factors, for example, material attributes, process parameters and machine capacities have a genuine impact on nature of items, in this way, such a significant number of the dialogue are required as for the working conditions [3, 19-23]. Micro gears and other strong parts have been manufactured utilizing micro bulk-forming [24]. Yet, conventional plastic shaping techniques have numerous hindrances impeding their application in micro-producing. It is difficult to make a micro die or mold, and, regardless of whether that exertion is effective, demolding turns into the issue. The spring-back wonder is one more issue that genuinely diminishes fabricating accuracy [2, 25]. Laser shock forming - a non-warm laser forming strategy that has the upsides of non-contact, apparatus-free, high efficiency, and high accuracy- has been effectively brought into micro-producing and has been accounted for as having incredible significance [26-31]. For the most part, there are two classes of laser shock forming: with mold [26] and without mold [2, 30, 31]. For the previous, the maximal flat size of the formed microstructure is dictated by the mold, and the laser parameters are the fundamental influence of the vertical size. For the last mentioned, the forming procedure is achieved without a mold, so the sizes of the shocked zones are for the most part dictated by the laser parameters. Laser shock forming without mold is free of all issues coming about because of micro molds. What's more, improvements in laser innovation empower limiting the energy to a little, localized region and inducing highly localized plastic deformation, which may expand the forming accuracy of the mold-free laser shock forming technique. Along these lines, mold-free forming innovation has extraordinary potential as an application in microfabrication. As of recently, ns lasers have been generally utilized in laser shock microforming [5-9]. Truth be told, fs lasers with shorter beats can induce shock waves with a lot higher pressure than ns lasers. For direct ablation by fs laser, tough shock wave with a peak pressure of tens to many GPa can without much of a stretch be acquired [32-35]. We likewise quantitatively assessed the peak pressure of an fs laser-induced shock wave when it was utilized for confined ablation (where a straightforward confining layer is utilized to confine the development of the ablated plasma) and we observed that, even with a very low laser fluence, the peak pressure could achieve a few many GPa [15], which is a lot higher than the dynamic yield qualities of general metals. In this way, fs laser-induced shock waves have been utilized in processing materials and creating parts [31, 36-41]. Contrasted with an ns laser, an fs laser has one of a kind focal points when performing micromachining and microfabricating, including higher exactness and the absence of a heat-affected zone [42, 43]. Additionally, due to the ultrashort stacking time, the all-out shock impact induced by an fs laser is not enormous enough to overwhelm microparts or burst thin metal goals [40, 41]. Every one of these properties makes fs lasers truly reasonable for micro-forming.

The purpose of this study is to review the Laser shock forming process on various types of materials using laser energy and also to introduce a new technology that could be used to produce microproducts at a cheaper cost. The deformation performances as influenced by laser handling parameters, including intensity of the laser, material thickness, tracks the number of scanning and covering ratio is revised. In addition, the ongoing advances in femtosecond LSMF and heat-assisted LSMF are studied.

### **1.1 A proposed cavitation water jet impact on microforming process (novelty).**

Based on the above research status and achievements, this paper proposes a new process of cavitation water jet impact metal foil micro-forming, which uses the high-energy impact of cavitation bubble collapse in the cavitation water jet to micro-form the metal foil. Water jet cavitation shock microforming has the advantages of low cost, good processing flexibility, and dramatically improved formability. Both cavitation water jet impact strengthening and impact microforming use the shock wave effect generated by the collapse of cavitation bubbles to exert mechanical force on the surface of the part, but their boundary conditions are different. For the former, the component is placed on a rigid substrate, the displacement of the bottom of the component is zero, and the plastic strain mainly occurs on the top surface of the material. For the latter, the part is clamped by two metal plates, which have the same axial hole at the centre, and the bottom surface is free, causing plastic deformation in all affected areas. Essentially, the difference between cavitation water jet impact microforming and impact strengthening is whether there is a constraint on the processed part in the forming direction. The

release of the constraint provides space for the forming of the workpiece. The comparison between them is shown in Figure 1.

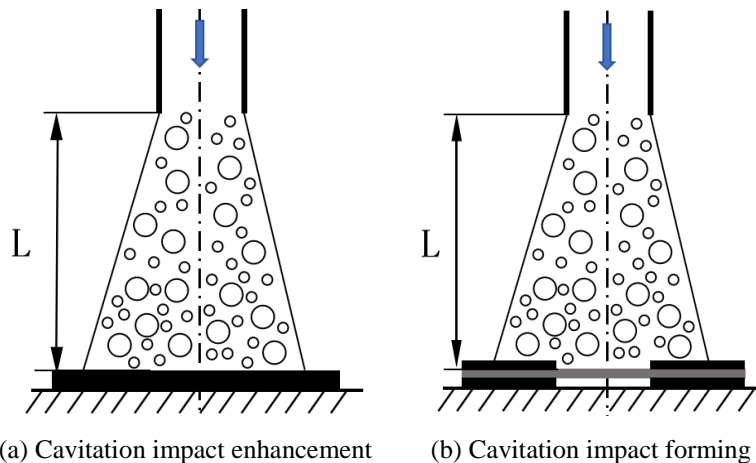


**Fig.1** Comparison between cavitating water jet impingement and impingement forming

## II. Laser Shock Micro-Forming process (LSMF)

### 2.1. Designing process

The experimental setup of the LSMF process is illustrated whereby Fig.2 (a) demonstrates that the laser pulse was led to the communication region by methods for a reflecting mirror and a centring focal point. The spot size can be balanced by changing the defocusing of the laser beam. The difference in the defocusing could be accomplished by modifying the working platform. To get the ideal laser spot to cover the effect zone totally, the workpiece was put far from the concentration at the correct separation. In this investigation, the laser spot was around 3 mm. Fig. 2(b) additionally demonstrates the essential idea of the laser shock forming process schematically. The tooling set comprises the confining medium, ablative medium, soft punch, thin metal sheet and unbending mold [44-46]. The confining medium could delay plasma development, improve energy coupling and postpone the shock wave time. The ablative medium can well secure the soft punch and significantly improve the absorption rate of the laser energy pulse. The soft punch can regulate and amplify pressure and it can undoubtedly isolate from the workpiece in the wake of forming activity without unreasonable force for the division. At the point when the laser pulse infiltrates the confining medium and lights the ablative medium on the soft punch, the ablative medium will be warmed and vaporized momentarily. The vapor ingests the rest of the laser energy and gets ionized into plasma with ultrahigh pressure. The plasma expands quickly and will be bounced back by the confining medium conveying a strong shockwave, which spreads into the soft punch, and the soft punch would have a solid flexible misshapen under the effect of the solid shock wave. For the flexible elastic material that has incompressible and hyperelastic attributes, the workpiece would be stacked by the soft punch in the following minute. Because of the imperative of mold, plastic deformation and shear stress are created in the objective area of the workpiece. Compression commands over the affected zone and the bending and pivotal extending of the workpiece would happen. As the affected zone moves to descend, the centre area of the thin metal foil is deformed conformal to the basic three-dimensional unbending mold under the strong shockwave pressure. Shear stresses are created through the objective thickness around the bend of the smaller micromold. In the end, shear and compression will offer an approach to bending and afterwards axial stretching. An objective plate will be sheared off around, along these lines the part is figured out. From the above depiction, it very well may be seen that in this forming procedure, just a single basic advance is required to manufacture a complex part [47-49].

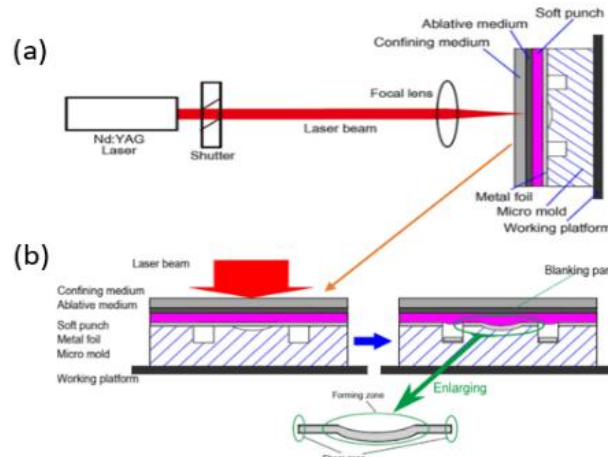


Fig. 2. (a) The layout of the experiment (b) The Diagrammatic illustration of the setup of the laser shock forming process [47].

## 2.2. Laser forming mechanisms

During the LSMF process, when a high-energy short-pulse laser beam is coordinated onto the sheet metal surface, the surface material is promptly vaporized and ionized [50-52]. This produces a high-pressure plasma, expanding quickly far from the sheet metal surface. Presenting a confining medium like water will trap the expanding plasma and re-direct it toward the sheet metal, where it viciously detonates against the surfaces of the metal sheet and control [53-55]. This entanglement essentially increases the pressure to a few GPa, inducing a shockwave propagated in the material [18, 53-56]. As the laser shockwave engenders into the workpiece, the peening impact presents surface compressive residual stresses [57-60]. The link between the shockwave pressure and the plastic deformation has been explored broadly [61-64]. During laser-material collaborations, plastic disfigurements will happen if the peak pressure of the laser-induced shockwave is more prominent than the Hugoniot elastic point of confinement (HEL) of the sample [65], as appeared in Fig. 3(a). Generally, plastic deformation increases straightly with the shockwave pressure inside the 1 HEL and 2 HEL range, which is the standard working condition for LSMF [66]. Inside this working state, the components of concave and convex bending have been investigated and are ascribed to the ratio of compressive residual stress entrance depth to the thickness of the sample material. Once the shockwave pressure outperforms the HEL, plastic disfigurement will occur underneath the laser-analyzed zone. Subsequently, the material structures using compressive residual stress inside this area have appeared in Fig. 3(b). The entrance depth of the compressive residual stress is dictated by the energy of the laser pulse and the properties of the objective material. By and large, the higher the intensity of the laser pulse, the deeper the compressive residual stress infiltrates into the objective material until an immersion point is reached [67-69].

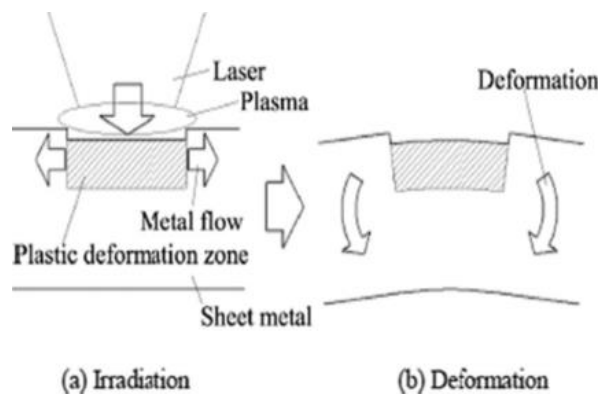


Fig. 3. Principle of LSMF during (a) irradiation and (b) deformation stages, adopted with permission from [50, 69].

### 2.3. Laser and material type

For a particular material with a given thickness, a key parameter administering the heading of the bend is laser intensity, pulse length etc. All the researchers used different intensities for their various studies and they are stated under various works reviewed [69]. Several research tests have been directed to explore how different materials and their thickness influence the forming or bending angle [69]. This is demonstrated in Table 1.

**Table 1 Various laser shock forming and its materials.**

Ref.	Laser type	Pulse energy (mJ)	Laser wavelength	Laser intensity	Pulse width	Material	Thickness (mm or $\mu\text{m}$ )	Die diameter
[70]2002	Q-switched	20ns	1.064	10 - 30	20	Ferritic stainless steel	0.3-10	
[71, 72]2005	Excimer Spotlight 2000 Nd:	20ns	248	6.4	250	Stainless steel AL99.5	50	1.4
[73]2017	YAG GAIN Nd:	80-2000	1064	1.6 & 2.0	8	Stainless steel	40, 60	1.2
[74]2016	YAG	2-9	1064	5.6	10	Aluminum	17	1.6
[13]2015	A Q-Switched Nd: YAG	2-9	1064	5.6	8	Titanium	35	1.6
[2]2013		75	1.064	5.2	38	Annealed copper Aluminium, copper, stainless steel	25	
[9]2008	TEA-CO2	3	10600		25, 700, 9		20, 50	
[75]2007	Nd: YAG	1		6	10	Copper	15	$B_d = 0.03$

### III. Experimental and theoretical investigations on the materials

This segment presents astounding experimental and theoretical investigations that have been directed in the field of laser shockmicroforming on ferrous, non-ferrous and advanced engineering materials. The significant examinations have been classified toward the finish of every subsection.

#### 3.1. Stainless steel

Steel is a standout amongst the most well-known materials on the planet and is utilized through the development of numerous design manufacturers. Many sub-classifications of steel rely upon the different characteristics and qualities of a specific form. The properties that shift the most between steel types are quality, pliability, hardness, style, and cost [76]. Notwithstanding the high production cost, the control of the forming quality is another test. Firstly, because of the expanding uses of lightweight metals, which by and large have relatively poor room temperature formability contrasted with mild steel [77] the sheet metal will in general neck or tear at moderately low strain levels, making the forming of complex parts problematic. Secondly, it is hard to efficiently control the wrinkling of the sheet zone without typical imperative, particularly for sheet metal parts with exceptionally thin-walled [77, 78]. Laser shock forming innovation for micro-sheet forming has been the subject of various examinations. The use of laser shock waves for metal sheets was endeavored by Zhou et al. [70]. Zhou et al. [79, 80] conducted a study on the deformation of 0.3 – 0.9-mm-thick austenitic and ferritic stainless steel sheets utilizing laser-prompted shock waves. Hence, the forming conducted in the laser extend forming procedure was examined by Niehoff SHand Coe workers[71]. Laser-induced stretch-forming tests were completed with a variation of the parameters defocusing, water height, number of pulses, power density and material. The utilized excimer laser has a wavelength of 248 nm and a pulse length of 20 ns. The most extreme pulse energy is 250mJ and the greatest power density is 6.4 GW/cm<sup>2</sup>, whereby a power density of 0.1 GW/cm<sup>2</sup> is adequate to touch off a plasma [72]. The arch height of the laser stretch-formed parts was utilized as a level of forming, assuming a uniform vault shape. They reported on a dynamic ultrahigh-strain-rate shaping technique driven by laser impact. This examination uncovers that laser shock forming is a mechanical, not a thermal procedure, and the strain rate can go up to 10<sup>7</sup>–10<sup>9</sup> s<sup>-1</sup>, two or more requests higher than that of all the current forming techniques. By exploring the hardness and residual stress of the surfaces, they concluded that laser shock forming is a strategy with joining laser shock strengthening and metal forming, which presents strain hardening and compressive residual stresses. They additionally found some nonlinear plastic deformation characters in laser shock forming [80]. Chi-Han Chen [81] also conducted an experimental and analytical study on the limit drawing ratio of Stainless Steel 304 foils on micro sheet forming. Stainless steel 304 foils with four thicknesses (150 $\mu\text{m}$ , 100 $\mu\text{m}$ , 50 $\mu\text{m}$ , and 20 $\mu\text{m}$ ) annealed at four distinct temperatures (900°C, 950°C, 1000°C, and 1050°C) for 3 minutes were utilized for this investigation. The motivation behind this examination is to find the influences of foil thickness, ordinary plastic anisotropy, grain size, and T/D proportion (thickness to average



grain measure proportion) on the LDR of treated steel 304 foils micro deep drawing. The experimental outcomes of this examination were likewise contrasted and two understood and acknowledged full-scale observational equations to find the restrictions of these two equations' application on the deep drawing. The experimental consequences of this examination can be utilized to not just find the use confinement of macro experiential equations yet, in addition, make the observational equations for micro deep drawing attracting what's to come[81].The punch with 2mm diameter ( $D_p$ ) and 0.25mm punch tip radius ( $R_p$ ) was utilized for analyses. Four unique dies were utilized in the examination. Die diameter ( $D_d$ ) is  $(1.1 \times \text{foil thickness } (\tau) \times 2 + D_p$ , and the relative die shoulder radius ( $R_d$ ) is four multiple times the foil thickness. For their investigation, the punch travel speed was set as 0.1 mm/sec, and the absolute deep drawing stroke is 2mm. Punch surface and die inward surface was cleaned, and no lubrication was utilized during the experiment. Their results of the tensile test of this investigation were recorded in Table 2 in which tensile strengths, normal plastic anisotropy ratios and yield strengths, defined as  $\bar{R} = (R_0 + 2R_{45} + R_{90})/4$ , of the foils ,can be observed. Clearly tensile strengths and yield strengths of the foils (150um, 100um, 50um, and 20um) decline with the increments of the annealing temperature (900°C, 950°C, 1000°C, and 1050°C). Because of work hardening, the as-got foils have bigger yield and tensile strengths than others even though they have bigger grain sizes than the foils annealed at 900°C.  $R_0$ ,  $R_{45}$ , and  $R_{90}$ of the foils were determined by estimating the micro-grids on tensile test examples cut along the rolling, diagonal (45°), and transverse ways, separately, and they are appeared Table 3. Too known in macroscale sheet metal forming,  $\bar{R}$  is a pointer of diminishing opposition: the higher the  $\bar{R}$  value is, the better the diminishing obstruction is. As appeared in Table 2, the normal plastic anisotropy  $\bar{R}$  for the foils with 150um and 100um thicknesses increased with the increments of annealing temperature. At the end of the day, for 150um and 100um foils, the  $\bar{R}$  value increased as T/D ratiodecreased. However, this pattern cannot be useful to the foils with 50um and 20um thicknesses. By observing Table 3, it very well may be seen that for the foils annealed at a similar temperature the  $\bar{R}$  increased as thickness decreased. This can likewise be translated that the R increased as T/D ratio decreased for the foils annealed at a similar temperature. The main special case is for the foils annealed at 950°C with 150um and 100um thicknesses. Since the thing that matters is just 0.003, this pattern might be pertinent to 950°C[81].

**Table 2 mechanical properties for stainless steel 304 foils [72, 81, 82]**

Heat treatment temperature ( $\tau$ ) (°C)	Yield strength (MPa)	Tensile strength (MPa)	$\bar{R}$	Yield strength (MPa)	Tensile strength (MPa)	$\bar{R}$
Blank thickness ( $\tau$ )		150um			100um	
1060	303.86	787.99	0.975	298.20	746.47	1.020
1000	328.19	806.55	0.878	324.75	771.26	0.800
950	350.34	827.77	0.798	355.96	806.73	0.795
900	368.69	857.74	0.563	516.15	906.59	0.578
As-received*	730.1	1188.9	-	821.5	1233.9	-
		50um			20um	
1060	316.61	728.31	1.108	378.48	636.62	1.178
1000	338.77	770.33	0.885	395.89	673.11	0.955
950	375.06	831.92	0.930	457.23	692.91	1.073
900	523.69	897.04	0.748	660.33	903.02	1.310
As-received*	1090.4	1301.6	-	1470.6	1470.6	-

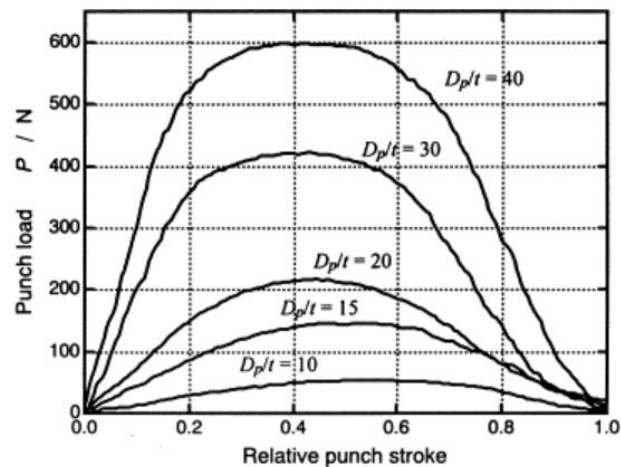
\*The results of the as-received materials were published in ICTP[72, 81, 82]

**Table 3 Plastic anisotropy ratio for stainless steel 304 foils [72, 81, 82]**

Heat treatment temperature ( $\tau$ ) (°C)	Blank thickness ( $\tau$ ) ( $\mu\text{m}$ )	$R(0^\circ)$	$R(90^\circ)$	$R(45^\circ)$	$\bar{R}$
1060	150	1.08	0.66	1.08	0.975
	100	1.32	0.86	0.95	1.020
	50	0.98	0.87	1.29	1.108
	20	2.50	0.69	0.76	1.178
1000	150	0.96	0.75	0.90	1.878
	100	0.97	0.69	0.77	0.800
	50	1.11	0.53	0.95	0.885
	20	2.00	0.66	0.58	0.955

950	150	1.13	0.94	0.56	0.798
	100	1.25	0.71	0.61	0.795
	50	1.70	0.56	0.73	0.930
	20	2.06	0.54	0.85	1.073
900	150	1.02	0.37	0.43	0.563
	100	0.96	0.41	0.47	0.578
	50	1.16	0.53	0.65	0.748
	20	2.30	0.74	1.10	1.310

To examine the micro-deep drawing process, Saotome and co-researchers [21] led probes of the steel with thicknesses from 0.05mm to 1mm. They utilized the relative punch diameter (punch diameter/thickness of sheet material) as a significant exploratory parameter to decide drawability. This drawability was assessed, and the similitude laws in deep drawing were analyzed with sheet steels of 0.05, 0.1, 0.2 and 1.0 mm thickness. For  $D_p/t$  from 10 to 100, common drawability was obtained for flimsy sheet steels without a lot of clear holder pressure, and a reduction in estimation of the constraining drawing ratio was seen with an expansion in  $D_p/t$ . The results of the Drawing process found that the cutoff drawing ratio (LDR) reduces with the expansion of the relative punch diameter. With an expansion of  $D_p/t$ , the purpose of the most extreme punch load winds up unmistakable prior to the all-out punch stroke. Moreover, the most extreme punch burden is observed to be bigger and all the more generally circulated along the all-out punch stroke for  $R_d/t=2.5$  (Fig. 4) in examination with that for  $R_d/t=5.0$ . This conduct is unmistakably uncovered for  $D_p/t=40$  as appeared in Fig. 4 and can be ascribed to the bending and backward bending component close to the die corner [21].



[21]

Figure 4. Punch load–relative stroke curves for various conditions of  $D_p/t$ . SPCE,  $R_d/t=2.5$ ,  $\beta=2.0$ ,  $t=0.1\text{mm}$  [21]. Liu [73] conducted a study on Laser flexible shock micro-drawing (LFSM) on micro and nanofabrication technology, which joins laser dynamic shaping and flexible die forming, which is a sort of high strain rate miniaturized micro-forming. The LFSM of 304 stainless steel foils was explored and its thickness was 40 $\mu\text{m}$  and 60 $\mu\text{m}$ , respectively. Their exploratory and simulated results demonstrated that the drawing depth and thickness thinning rate of bulging parts expanded with an expansion of laser energy and a lessening of workpiece thickness. Experimental results likewise demonstrated the surface morphology of illustration parts. The surface morphology of the micro-bulging parts was observed through SEM, as shown in Figure 5. They discovered that the shape of the LFSM had a spherical surface when the workpiece thickness was larger and was a nearly spherical surface when it was small [73]. As per Figures 5 and 6(a), it was discovered that the depth of the micro drawing parts expanded with an expansion of the laser energy under a similar workpiece thickness; under similar laser energy, the depth of the micro drawing parts additionally expanded with an abatement of workpiece thickness. This marvel can be clarified by the surface layer model for the polycrystalline material [83].

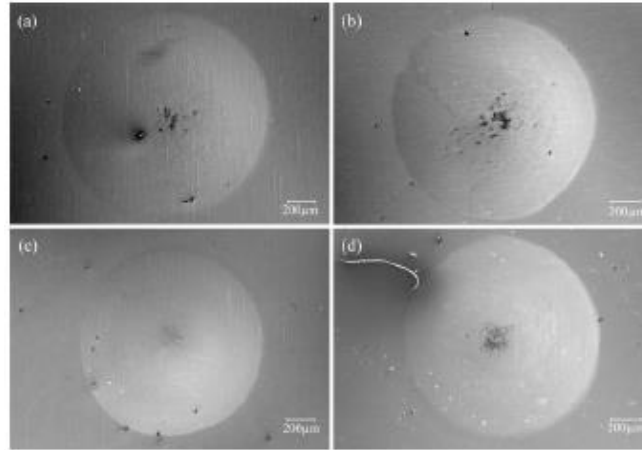


Fig. 5 The surface morphology of micro bulging parts under different conditions: (a) 60µm, 565mJ (b) 60µm, 835mJ (c) 40µm, 565mJ (d) 40µm, 835mJ[73].

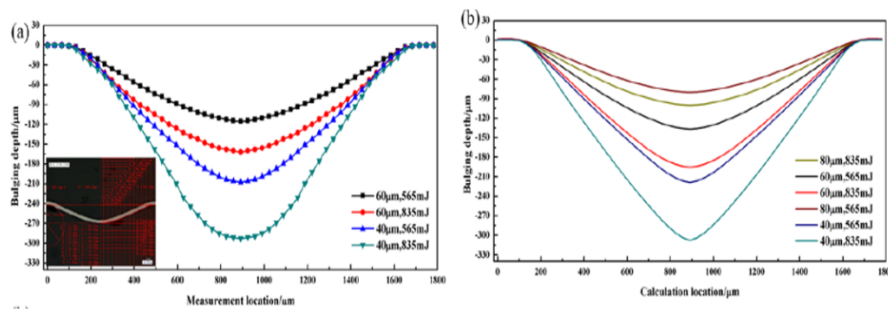


Fig. 6 The depth of the micro-bulging parts (a) experimental results (b) simulation results[73].

### 3.2. Aluminum and its alloys

Thin aluminium sheets have been utilized in the assembling of printed circuit boards(PCBs), and so forth. The aluminium sheet has inborn constraints, including high reflectivity, high warm conductivity, and the recognized oxidation response, as far as laser material handling[84, 85]. Aluminium and its combinations have been broadly utilized in different parts, for example, chemical industries, construction, spacecraft, automobiles and marine [86-88]. Zhang [74]performed laser shock micro-forming on a thin aluminium sheet having a thickness of 17 µm. Plasticine is utilized as the adaptable help to supplant other micro-mold. The physical science of the mold-free shock micro drawing forming procedure of metal foils is examined alongside the impact of the laser energy and material sort on deformation. The adjustment in material thickness after forming is concentrated to research the danger of cracking. Also, a 3×4 array of craters is manufactured to show the repeatability of this method. A computerized magnifying lens (KeyenceVHX-1000) was utilized to examine the three-dimensional morphologies of the micro-craters on the metal foil surfaces, just as the ablation condition of the ablative medium. Figure 3 demonstrates the diverse ablationconditions of the ablative mediums (aluminium foil) under various laserenergies. As appeared in Fig. 7(a–d), shows that the ablation conditions of ablative mediums would be progressively serious with the expanding laser pulse energies (from 1020 to 1900mJ). Furthermore, some seriousablation conditions could beobtainedwith1690mJ and1900mJ laser energies. Notwithstanding, the ablative mediums still stay unblemished without any crack apparentafter forming. This demonstrates the presence of the genuine ablation state would not havean unfavourable impact on workpiece quality.



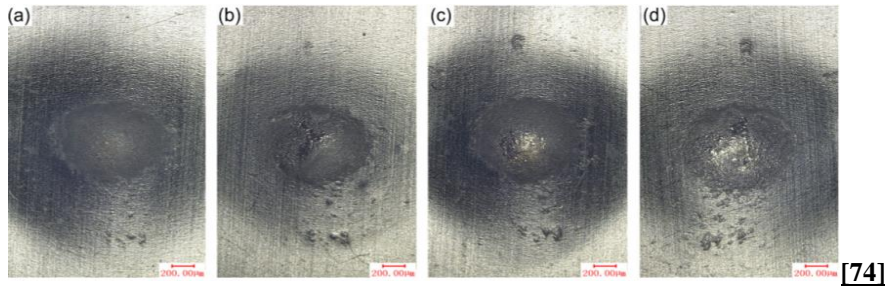


Fig.7 Theablationstatesofablative mediums(aluminiumfoil)with17- $\mu$ m-thickaluminiumfoilsasworkpieces:(a)with1020mJenergy,(b)with1380mJ energy, (c) with 1690mJ energy, and (d) with 1900mJ energy[74].

Zhang [74] also observed the influence of laser energy and material type. In the mold-free laser shock micro-drawing forming (MFLSMDF) process, a laser beam is utilized as the variable convex mold; the properties of which will have impacts on the crater profile. Along these lines, it is important to direct investigations to examine the effects of laser energy on the deformation of thin metal foils. The (MFLSMDF) procedure was performed on aluminium, titanium and copper foils. The tests were rehashed multiple times, and the normal qualities were embraced to draw Fig. 7. The outcomes obtained for a 17- $\mu$ m-thick aluminium foil workpiece appear in Fig. 8; the crater depths and widths increase with increasing laser energy from 1020 to 1900mJ. It is justifiable that the expansion of the micro-crater depth can be clarified by the expanded pressure[74].

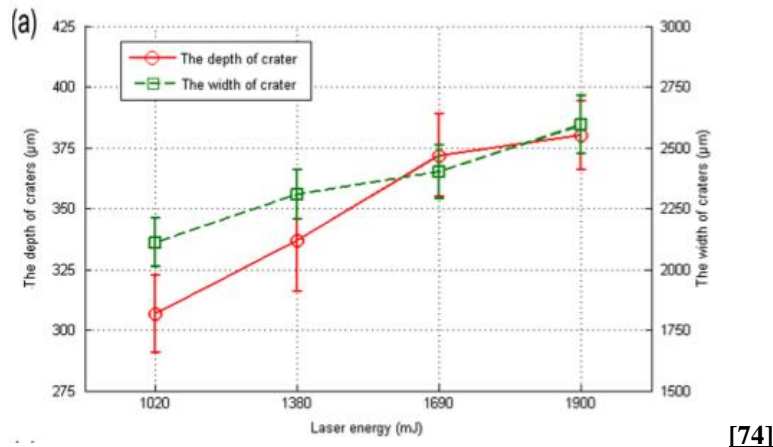


Fig. 8 The crater depth and crater width variation with increasing energies (1020mJ, 1380mJ, 1690mJ, and 1900mJ) for a laser on a 17 $\mu$ m-thick aluminium foil.

He also studied the 3D (three-dimensional) micro-topography of the workpiece. Figure 9(a & b) demonstrates the deliberate surface 3D micro-geography of the aluminium test in the laser shock area. It tends to be seen that a smooth crater was formed without any indications of burning, ablation, or melting, implying that the forming procedure is non-thermal. As observed, the sample creates plastic deformation and the workpiece has a high spatial goal at the micronlevel. The ablative medium can shield the workpiece from thermal impacts with the end goal that absolute mechanical impacts are induced [74].

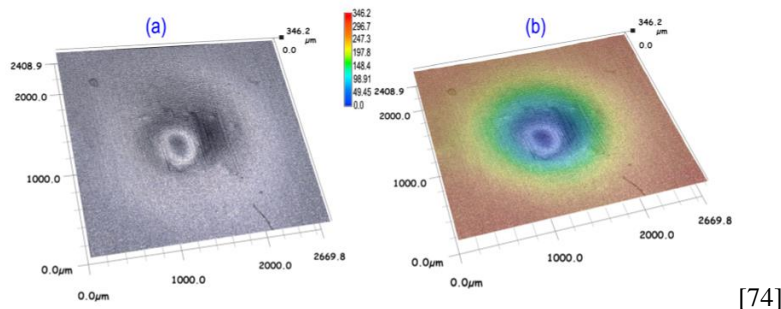


Fig. 9 Micro-crater in the shock region (a laser of 1020mJ energy on a 17- $\mu$ m-thick Al sample).  
 a) Themagnificationmicro-topographyofthe micro-crater; (b) 3D plot of the formed crater; (c) surface profile curve of the crater[74].

Figure 9c demonstrates the surface profile curve of the sample surface crater. The misshaping profundity must achieve 321.µm with the most extreme disfigurement depth happening at the centre of the crater. The disfigurement force applied to the metal foil depends on the laser-induced shock loading. Likewise, the formed micro-crater can expand the fatigue resistance of the workpiece.

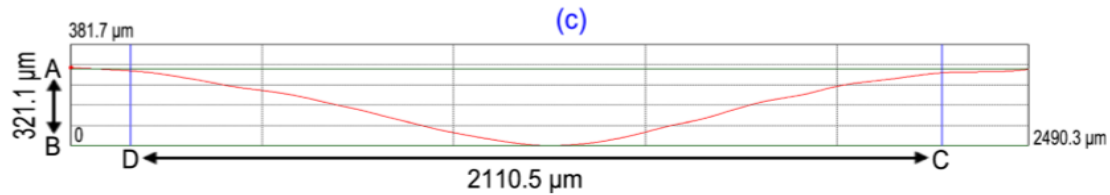
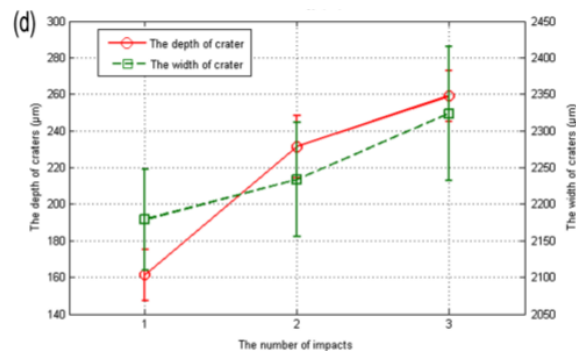


Fig.9c Surface profile curve[74].

### 3.3. Titanium and its alloys

Titanium shows poor wear resistance, and its weariness performance depends to an enormous degree on its surface properties [89]. The great mechanical properties, high strength-to-weight ratio, erosion-corrosion obstruction and non-danger make titanium a spine material for the armor, aviation, medical and automobile industries. Titanium and its alloys are utilized in assembling some substantial parts, for example, aircraft structure components, and aircraft turbine engine components [73, 90-96]. Because of the various significant mechanical properties of these materials, the various analysts have directed experiments just as theoretical examinations on the laser shock micro-forming of these materials.

Zhang [13] has performed LSMF on a thin titanium foil having a thickness of 35µm. The Plasticine is utilized as the adaptable help to supplant another micro mold. The physical science of the MFLSMDF procedure of metal foils is considered alongside the impact of the laser energy and material sort on misshaping. The adjustment in material thickness after forming is concentrated to explore the danger of cracking. Furthermore, a 3×4 array of the crater is manufactured to show the repeatability of this method. An advanced magnifying instrument (KeyenceVHX-1000) was utilized to break down the three-dimensional morphologies of the micro-craters on the metal foil surfaces, just as the ablation condition of the ablative medium. It would in this manner be valuable and interesting to examine the arrangement of micro-crater in titanium utilizing the mold-free laser shock micro-drawing forming process. We utilized 35µm-thick titanium foil as the workpiece. Various effects were applied to the titanium foil to acquire reasonable craters, as appeared in Fig 10[13].



[13]

Fig. 10 The crater depth and crater width variation with increasing impact numbers (1,2, and 3) for a laser on a 35-µm-thick titanium foil [13].

The 2D and 3D morphologies of the titanium workpiece after one effect appear in Figure 11, uncovering the high-surface nature of the workpiece. The forming depth of the crater came to almost 160µm and the width was around 2325µm. It tends to be expected that different deformations and crater profiles in various metal foils could be achieved by utilizing the technique for MFLSMDF basically by alteration of the laser handling parameters [13].

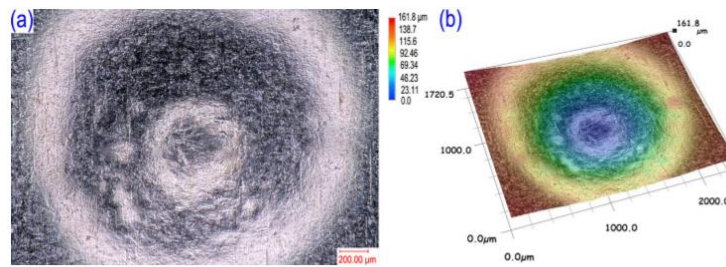


Fig. 11 The surface of titanium workpiece after one impact: a The magnification micro-topography of micro-crater; b 3D plot of the formed crater [13].

#### IV. Conclusions

The ongoing advancements in Laser Shock Forming (LSF) research was looked into with an accentuation on condensing the designing processes, forming mechanism, processing parameters, and experimental and theoretical experiments on various materials. The shaping mechanisms contributing to the forming were investigated exclusively by portraying the reaction of the framework to be applied. To empower modern uses of LSF and guarantee its viability, a procedure model fit for predicting bending practices of sheet metals is of explicit significance. An essential comprehension of the forming mechanisms, principles of laser, material interactions, superpose compressive stresses, variety of thicknesses and heat treatment temperatures, the blank holder forces on the micro deep drawing, the mechanical properties, surface roughness, surface morphology, forming depth, the microstructure, a new model of micro inhomogeneity of metal and an original algorithm to determine inhomogeneous parameters for prediction and predicted by the proposed FE model and effects of size consequences for formability and flow stress methodology. Based on the above research status and achievements, this paper proposes a new process of cavitation water jet impact metal foil micro-forming, which uses the high-energy impact of cavitation bubble collapse in the cavitation water jet to micro-form the metal foil. Water jet cavitation shock microforming has the advantages of low cost, good processing flexibility, and dramatically improved formability. Both cavitation water jet impact strengthening and impact microforming use the shock wave effect generated by the collapse of cavitation bubbles to exert mechanical force on the surface of the part, but their boundary conditions are different. For the former, the component is placed on a rigid substrate, the displacement of the bottom of the component is zero, and the plastic strain mainly occurs on the top surface of the material. For the latter, the part is clamped by two metal plates, which have the same axial hole at the centre, and the bottom surface is free, causing plastic deformation in all affected areas. Essentially, the difference between cavitation water jet impact microforming and impact strengthening is whether there is a constraint on the processed part in the forming direction were discussed in this review paper.

#### References

- [1]. A. Gillner, J. Holtkamp, C. Hartmann, A. Olowinsky, J. Gedicke, K. Klages, *et al.*, "Laser applications in microtechnology," *Journal of Materials Processing Technology*, vol. 167, pp. 494-498, 2005.
- [2]. B. Nagarajan, S. Castagne, and Z. Wang, "Mold-free fabrication of 3D microfeatures using laser-induced shock pressure," *Applied Surface Science*, vol. 268, pp. 529-534, 2013/03/01/ 2013.
- [3]. M. Geiger, M. Kleiner, R. Eckstein, N. Tiesler, and U. Engel, "Microforming," *CIRP Annals*, vol. 50, pp. 445-462, 2001/01/01/ 2001.
- [4]. Y. Q. Akhtar Razul Razali, "A review on micro-manufacturing, micro-forming and their key issues," *Procedia Engineering*, vol. 53, pp. 665-672, 2013.
- [5]. J.-T. Gau, S. Teegala, K.-M. Huang, T.-J. Hsiao, and B.-T. Lin, "Using micro deep drawing with ironing stages to form stainless steel 304 micro cups," *Journal of Manufacturing Processes*, vol. 15, pp. 298-305, 2013.
- [6]. M. Fu and W. Chan, "A review on the state-of-the-art microforming technologies," *The International Journal of Advanced Manufacturing Technology*, vol. 67, pp. 2411-2437, 2013.
- [7]. B. Joo, S. Oh, and Y. Son, "Forming of micro channels with ultra thin metal foils," *CIRP Annals*, vol. 53, pp. 243-246, 2004.
- [8]. H. Yin, Z. Jiang, H. Xie, F. Jia, X. Wang, and C. Zhou, "Micro forming of metallic composites," *Procedia Manufacturing*, vol. 15, pp. 1429-1436, 2018/01/01/ 2018.
- [9]. F. Vollertsen, H. S. Niehoff, and H. Wielage, "On the acting pressure in laser deep drawing," *Production Engineering*, vol. 3, p. 1, 2008/10/25 2008.
- [10]. H. Lu, D. Wei, Z. Jiang, X. Liu, and K. Manabe, "Modelling of size effects in microforming process with consideration of grained heterogeneity," *Computational Materials Science*, vol. 77, pp. 44-52, 2013.
- [11]. U. Engel and R. Eckstein, "Microforming—from basic research to its realization," *Journal of Materials Processing Technology*, vol. 125-126, pp. 35-44, 2002/09/09/ 2002.
- [12]. H. Zhang and X. Dong, "Physically based crystal plasticity FEM including geometrically necessary dislocations: numerical implementation and applications in micro-forming," *Computational Materials Science*, vol. 110, pp. 308-320, 2015.
- [13]. D. Zhang, Y. Lin, C. Gu, Z. Shen, H. Liu, and X. Wang, *A mold-free laser shock micro-drawing forming process using Plasticine as the flexible support* vol. 79, 2015.
- [14]. F. Vollertsen, "Metal forming: microparts," 2001.

- [15]. G.-Y. Kim, J. Ni, and M. Koç, "Modeling of the size effects on the behavior of metals in microscale deformation processes," *Journal of Manufacturing Science and Engineering*, vol. 129, pp. 470-476, 2007.
- [16]. B. Yilbas, S. Mansoor, and A. Arif, "Laser shock processing: modeling of evaporation and pressure field developed in the laser-produced cavity," *The International Journal of Advanced Manufacturing Technology*, vol. 42, pp. 250-262, 2009.
- [17]. S. G. Irizalp, N. Saklakoglu, and B. S. Yilbas, "Characterization of microplastic deformation produced in 6061-T6 by using laser shock processing," *The International Journal of Advanced Manufacturing Technology*, vol. 71, pp. 109-115, 2014.
- [18]. K. R. Edwards, S. P. Edwardson, C. Carey, G. Dearden, and K. G. Watkins, "Laser micro peen forming without a tamping layer," *The International Journal of Advanced Manufacturing Technology*, vol. 47, pp. 191-200, 2010.
- [19]. H. S. Niehoff and F. Vollertson, "Laser induced shock waves in deformation processing," *Metalurgija*, vol. 11, pp. 183-194, 2005.
- [20]. T. Furushima, T. Nakayama, and K. Sasaki, "A new theoretical model of material inhomogeneity for prediction of surface roughening in micro metal forming," *CIRP Annals*, 2019/05/17/ 2019.
- [21]. Y. Saotome, K. Yasuda, and H. Kaga, "Microdeep drawability of very thin sheet steels," *Journal of Materials Processing Technology*, vol. 113, pp. 641-647, 2001/06/15/ 2001.
- [22]. A. Jaisingh, K. Narasimhan, P. Date, S. Maiti, and U. Singh, "Sensitivity analysis of a deep drawing process for miniaturized products," *Journal of materials processing technology*, vol. 147, pp. 321-327, 2004.
- [23]. L. Peng, P. Hu, X. Lai, D. Mei, and J. Ni, *Investigation of micro/meso sheet soft punch stamping process – simulation and experiments* vol. 30, 2009.
- [24]. D. Wang, T. Shi, J. Pan, G. Liao, Z. Tang, and L. Liu, "Finite element simulation and experimental investigation of forming micro-gear with Zr-Cu-Ni-Al bulk metallic glass," *Journal of Materials Processing Technology*, vol. 210, pp. 684-688, 2010.
- [25]. T. Masuzawa, "State of the art of micromachining," *Cirp Annals*, vol. 49, pp. 473-488, 2000.
- [26]. C. Zheng, S. Sun, Z. Ji, W. Wang, and J. Liu, "Numerical simulation and experimentation of micro scale laser bulge forming," *International Journal of Machine Tools and Manufacture*, vol. 50, pp. 1048-1056, 2010/12/01/ 2010.
- [27]. J. Di, M. Zhou, J. Li, C. Li, W. Zhang, and G. Amoako, "Micro-punching process based on spallation delamination induced by laser driven-flyer," *Applied Surface Science*, vol. 258, pp. 2339-2343, 2012.
- [28]. C. Zheng, S. Sun, Z. Ji, and W. Wang, "Effect of laser energy on the deformation behavior in microscale laser bulge forming," *Applied Surface Science*, vol. 257, pp. 1589-1595, 2010.
- [29]. H. Schulze Niehoff and F. Vollertsen, "Non-thermal laser stretch-forming," in *Advanced Materials Research*, 2005, pp. 433-440.
- [30]. J. L. Ocaña, M. Morales, J. Porro, J. García-Ballesteros, and C. Correa, "Laser shock microforming of thin metal sheets with ns lasers," *Physics Procedia*, vol. 12, pp. 201-206, 2011.
- [31]. Y. Ye, Y. Feng, X. Hua, and Z. Lian, "Experimental research on laser shock forming metal foils with femtosecond laser," *Applied Surface Science*, vol. 285, pp. 600-606, 2013.
- [32]. J. Cuq-Lelandais, M. Boustie, L. Berthe, T. De Ressaiguier, P. Combis, J.-P. Colombier, *et al.*, "Spallation generated by femtosecond laser driven shocks in thin metallic targets," *Journal of Physics D: Applied Physics*, vol. 42, p. 065402, 2009.
- [33]. L. Huang, Y. Yang, Y. Wang, Z. Zheng, and W. Su, "Measurement of transit time for femtosecond-laser-driven shock wave through aluminium films by ultrafast microscopy," *Journal of Physics D: Applied Physics*, vol. 42, p. 045502, 2009.
- [34]. A. A. Ionin, S. I. Kudryashov, S. V. Makarov, L. V. Seleznev, and D. V. e. Sinityn, "Generation and detection of superstrong shock waves during ablation of an aluminum surface by intense femtosecond laser pulses," *JETP letters*, vol. 94, p. 34, 2011.
- [35]. N. Inogamov, V. Khokhlov, Y. Petrov, S. Anisimov, V. V. Zhakhovsky, B. J. Demaske, *et al.*, "Ultrashort elastic and plastic shockwaves in aluminum," in *AIP Conference Proceedings*, 2012, pp. 909-912.
- [36]. Y. Ye, Y. Feng, Z. Lian, and Y. Hua, "Plastic deformation mechanism of polycrystalline copper foil shocked with femtosecond laser," *Applied Surface Science*, vol. 309, pp. 240-249, 2014.
- [37]. H. Nakano, S. Miyauti, N. Butani, T. Shibayanagi, M. Tsukamoto, and N. Abe, "Femtosecond laser peening of stainless steel," *Laser Micro/Nanoeng*, vol. 4, pp. 35-38, 2009.
- [38]. D. Lee, "Feasibility Study on Laser Microwelding and Laser Shock Peening using Femtosecond Laser Pulses," 2008.
- [39]. B. Wu, S. Tao, and S. Lei, "Numerical modeling of laser shock peening with femtosecond laser pulses and comparisons to experiments," *Applied Surface Science*, vol. 256, pp. 4376-4382, 2010.
- [40]. Y. Sagisaka, "Micro forming using shock wave generated by femtosecond laser irradiation," *기타자료*, pp. 719-719, 2008.
- [41]. Y. Sagisaka, M. Kamiya, M. Matsuda, and Y. Ohta, "Thin-sheet-metal bending by laser peen forming with femtosecond laser," *Journal of Materials Processing Technology*, vol. 210, pp. 2304-2309, 2010.
- [42]. B. N. Chichkov, C. Momma, S. Nolte, F. Von Alvensleben, and A. Tünnermann, "Femtosecond, picosecond and nanosecond laser ablation of solids," *Applied Physics A*, vol. 63, pp. 109-115, 1996.
- [43]. X. Zhu, D. Villeneuve, A. Y. Naumov, S. Nikumb, and P. Corkum, "Experimental study of drilling sub-10  $\mu\text{m}$  holes in thin metal foils with femtosecond laser pulses," *Applied Surface Science*, vol. 152, pp. 138-148, 1999.
- [44]. N. Shen, H. Ding, Q. Wang, and H. Ding, "Effect of confinement on surface modification for laser peen forming without protective coating," *Surface and Coatings Technology*, vol. 289, pp. 194-205, 2016.
- [45]. Y. Guo and R. Caslaru, "Fabrication and characterization of micro dent arrays produced by laser shock peening on titanium Ti-6Al-4V surfaces," *Journal of Materials Processing Technology*, vol. 211, pp. 729-736, 2011.
- [46]. J. J. Ruschau, R. John, S. R. Thompson, and T. Nicholas, "Fatigue crack nucleation and growth rate behavior of laser shock peened titanium," *International Journal of Fatigue*, vol. 21, pp. S199-S209, 1999.
- [47]. X. Wang, D. Zhang, C. Gu, Z. Shen, Y. Ma, Y. Gu, *et al.*, "Micro scale laser shock forming of pure copper and titanium sheet with forming/blanking compound die," *Optics and Lasers in Engineering*, vol. 67, pp. 83-93, 2015/04/01/ 2015.
- [48]. X. Wang, D. Du, H. Zhang, Z. Shen, H. Liu, J. Zhou, *et al.*, "Investigation of microscale laser dynamic flexible forming process—Simulation and experiments," *International Journal of Machine Tools and Manufacture*, vol. 67, pp. 8-17, 2013.
- [49]. H. Liu, J. Li, Z. Shen, Q. Qian, H. Zhang, and X. Wang, "Experimental and numerical simulation research on micro-gears fabrication by laser shock punching process," *Micromachines*, vol. 6, pp. 969-983, 2015.
- [50]. Y. Sagisaka, M. Kamiya, M. Matsuda, and Y. Ohta, "Application of Femtosecond Laser Peen Forming to Sheet Metal Bending," *Journal of Laser Micro/Nanoengineering*, vol. 7, 2012.
- [51]. B. Wu and Y. C. Shin, "A one-dimensional hydrodynamic model for pressures induced near the coating-water interface during laser shock peening," *Journal of applied physics*, vol. 101, p. 023510, 2007.
- [52]. Y. Sagisaka, K. Yamashita, W. Yanagihara, and H. Ueta, "Microparts processing using laser cutting and ultra-short-pulse laser peen forming," *Journal of Materials Processing Technology*, vol. 219, pp. 230-236, 2015.
- [53]. C. Montross, V. Florea, and J. Bolger, "Laser-induced shock wave generation and shock wave enhancement in basalt," in *International Journal of Rock Mechanics and Mining Sciences and Geomechanics Abstracts*, 1999, pp. 849-855.



- [54]. G. Tani, L. Orazi, A. Fortunato, A. Ascari, and G. Campana, "Warm laser shock peening: New developments and process optimization," *CIRP annals*, vol. 60, pp. 219-222, 2011.
- [55]. A. H. Clauer, J. H. Holbrook, and B. P. Fairand, "Effects of laser induced shock waves on metals," in *Shock waves and high-strain-rate phenomena in metals*, ed: Springer, 1981, pp. 675-702.
- [56]. Y. Wang, Y. Fan, S. Vukelic, and Y. L. Yao, "Energy-level effects on the deformation mechanism in microscale laser peen forming," *Journal of Manufacturing Processes*, vol. 9, pp. 1-12, 2007.
- [57]. C. S. Montross, T. Wei, L. Ye, G. Clark, and Y.-W. Mai, "Laser shock processing and its effects on microstructure and properties of metal alloys: a review," *International Journal of Fatigue*, vol. 24, pp. 1021-1036, 2002/10/01/ 2002.
- [58]. H. Tanaka, K. Akita, Y. Sano, and S. Ohya, "Compressive residual stress generation process by laser peening without pre-coating," *WIT Transactions on The Built Environment*, vol. 85, 2006.
- [59]. J. Im, R. V. Grandhi, and Y. Ro, "Residual stress behaviors induced by laser peening along the edge of curved models," *Journal of mechanical science and technology*, vol. 26, pp. 3943-3952, 2012.
- [60]. G. Gomez-Rosas, C. Rubio-Gonzalez, J. Ocana, C. Molpeceres, J. Porro, W. Chi-Moreno, *et al.*, "High level compressive residual stresses produced in aluminum alloys by laser shock processing," *Applied Surface Science*, vol. 252, pp. 883-887, 2005.
- [61]. P. Peyre, L. Berthe, V. Vignal, I. Popa, and T. Baudin, "Analysis of laser shock waves and resulting surface deformations in an Al-Cu-Li aluminum alloy," *Journal Of Physics D: Applied Physics*, vol. 45, p. 335304, 2012.
- [62]. C.-j. Yang, Y.-k. Zhang, J.-z. Zhou, M.-x. Ni, J.-j. Du, S. Huang, *et al.*, "Analysis and experiment on deformation of sheet metal by laser shock wave," *Frontiers of Mechanical Engineering in China*, vol. 1, pp. 448-451, 2006.
- [63]. B. Yilbas, A. Arif, and M. Gondal, "Plastic deformation of steel surface due to laser shock processing," *Proceedings of the Institution of Mechanical Engineers, Part B: Journal of Engineering Manufacture*, vol. 220, pp. 857-867, 2006.
- [64]. A. F. M. Arif, "Numerical prediction of plastic deformation and residual stresses induced by laser shock processing," *Journal of Materials Processing Technology*, vol. 136, pp. 120-138, 2003.
- [65]. C. Ye and G. J. Cheng, "Effects of temperature on laser shock induced plastic deformation: the case of copper," *Journal of manufacturing science and engineering*, vol. 132, p. 061009, 2010.
- [66]. H. Ding, N. Shen, K. Li, W. Bo, C. N. Pence, and H. Ding, "Experimental and numerical analysis of laser peen forming mechanisms of sheet metal," in *ASME 2014 International Manufacturing Science and Engineering Conference collocated with the JSME 2014 International Conference on Materials and Processing and the 42nd North American Manufacturing Research Conference*, 2014, pp. V002T02A102-V002T02A102.
- [67]. C. Ziwen, X. Haiying, Z. Shikun, and C. Zhigang, "Investigation of surface integrity on TC17 titanium alloy treated by square-spot laser shock peening," *Chinese Journal of Aeronautics*, vol. 25, pp. 650-656, 2012.
- [68]. W. Zhang, J. Lu, and K. Luo, "Residual stress distribution and microstructure at a laser spot of AISI 304 stainless steel subjected to different laser shock peening impacts," *Metals*, vol. 6, p. 6, 2015.
- [69]. C. J. Yocom, X. Zhang, and Y. Liao, "Research and development status of laser peen forming: A review," *Optics & Laser Technology*, vol. 108, pp. 32-45, 2018/12/01/ 2018.
- [70]. J. Zhou, J. Yang, Y. Zhang, and M. Zhou, "A study on super-speed forming of metal sheet by laser shock waves," *Journal of Materials Processing Technology*, vol. 129, pp. 241-244, 2002.
- [71]. V. F. Niehoff SH, "Laser induced shock waves in deformation processing," *Metalurgija*, vol. 11, pp. 183-194, 2005.
- [72]. H. Hügel, "Laser für die Materialbearbeitung," in *Strahlwerkzeug Laser*, ed: Springer, 1992, pp. 123-176.
- [73]. H. Liu, X. Sun, Z. Shen, L. Li, C. Sha, Y. Ma, *et al.*, *Experimental and Numerical Simulation Investigation on Laser Flexible Shock Micro-Bulging* vol. 7, 2017.
- [74]. J. Li, H. Liu, Z. Shen, Q. Qian, H. Zhang, and X. Wang, "Formability of micro-gears fabrication in laser dynamic flexible punching," *Journal of Materials Processing Technology*, vol. 234, pp. 131-142, 2016.
- [75]. G. J. Cheng, D. Pirzada, and Z. Ming, "Microstructure and mechanical property characterizations of metal foil after microscale laser dynamic forming," *Journal of applied physics*, vol. 101, p. 063108, 2007.
- [76]. H. Zhang, M. Zhou, Y. Wang, X. Zhang, Y. Yan, and R. Wang, "Development of a quantitative method for the characterization of hole quality during laser trepan drilling of high-temperature alloy," *Applied Physics A*, vol. 122, p. 74, 2016.
- [77]. Y.-Z. Chen, W. Liu, Y.-C. Xu, and S.-J. Yuan, "Analysis and experiment on wrinkling suppression for hydroforming of curved surface shell," *International Journal of Mechanical Sciences*, vol. 104, pp. 112-125, 2015.
- [78]. W. Liu, Y. Xu, and S. Yuan, "Effect of pre-bulging on wrinkling of curved surface part by hydromechanical deep drawing," *Procedia Engineering*, vol. 81, pp. 914-920, 2014.
- [79]. M. Zhou, Y. Zhang, and L. Cai, "Laser shock forming on coated metal sheets characterized by ultrahigh-strain-rate plastic deformation," *Journal of applied physics*, vol. 91, pp. 5501-5503, 2002.
- [80]. M. Zhou, Y. Zhang, and L. Cai, "Ultrahigh-strain-rate plastic deformation of a stainless-steel sheet with TiN coatings driven by laser shock waves," *Applied Physics A*, vol. 77, pp. 549-554, 2003.
- [81]. C.-H. Chen, J.-T. Gau, and R.-S. Lee, "An experimental and analytical study on the limit drawing ratio of stainless steel 304 foils for microsheet forming," *Materials and Manufacturing Processes*, vol. 24, pp. 1256-1265, 2009.
- [82]. R.-S. Lee, C.-H. Chen, and J.-T. Gau, "Effect of thickness to grain size ratio on drawability for micro deep drawing of AISI 304 stainless steel," in *Proceeding of International Conference on Technology of Plasticity, Gyeongju, Korea*, 2008.
- [83]. M. Geiger, F. Vollertsen, and R. Kals, "Fundamentals on the manufacturing of sheet metal microparts," *CIRP annals*, vol. 45, pp. 277-282, 1996.
- [84]. A. Dinsdale and P. Quedsted, "The viscosity of aluminium and its alloys--A review of data and models," *Journal of materials science*, vol. 39, pp. 7221-7228, 2004.
- [85]. X.-F. Xia, Y.-Y. Gu, and S.-A. Xu, "Titanium conversion coatings on the aluminum foil AA 8021 used for lithium-ion battery package," *Applied Surface Science*, vol. 419, pp. 447-453, 2017.
- [86]. G. Norkey, A. K. Dubey, and S. Agrawal, "Artificial intelligence based modeling and optimization of heat affected zone in Nd: YAG laser cutting of duralumin sheet," *Journal of Intelligent & Fuzzy Systems*, vol. 27, pp. 1545-1555, 2014.
- [87]. P. Santa Coloma, U. Izagirre, Y. Belaustegi, J. Jorcin, F. Cano, and N. Lapeña, "Chromium-free conversion coatings based on inorganic salts (Zr/Ti/Mn/Mo) for aluminum alloys used in aircraft applications," *Applied Surface Science*, vol. 345, pp. 24-35, 2015.
- [88]. S.-A. Xu, S.-N. Wang, and Y.-Y. Gu, "Microstructure and adhesion properties of cerium conversion coating modified with silane coupling agent on the aluminum foil for lithium ion battery," *Results in Physics*, vol. 13, p. 102262, 2019/06/01/ 2019.
- [89]. H. Liu, Y. Hu, X. Wang, Z. Shen, P. Li, C. Gu, *et al.*, "Grain refinement progress of pure titanium during laser shock forming (LSF) and mechanical property characterizations with nanoindentation," *Materials Science and Engineering: A*, vol. 564, pp. 13-21, 2013.



- [90]. A. K. Pandey and A. K. Dubey, "Multiple quality optimization in laser cutting of difficult-to-laser-cut material using grey–fuzzy methodology," *The International Journal of Advanced Manufacturing Technology*, vol. 65, pp. 421-431, 2013.
- [91]. A. K. Pandey and A. K. Dubey, "Modeling and optimization of kerf taper and surface roughness in laser cutting of titanium alloy sheet," *Journal of mechanical science and technology*, vol. 27, pp. 2115-2124, 2013.
- [92]. A. K. Pandey and A. K. Dubey, "Fuzzy expert system for prediction of kerf qualities in pulsed laser cutting of titanium alloy sheet," *Machining Science and Technology*, vol. 17, pp. 545-574, 2013.
- [93]. G. D. Gautam and A. K. Pandey, "Pulsed Nd:YAG laser beam drilling: A review," *Optics & Laser Technology*, vol. 100, pp. 183-215, 2018/03/01/ 2018.
- [94]. E. Maawad, Y. Sano, L. Wagner, H.-G. Brokmeier, and C. Genzel, "Investigation of laser shock peening effects on residual stress state and fatigue performance of titanium alloys," *Materials Science and Engineering: A*, vol. 536, pp. 82-91, 2012.
- [95]. C. Le, Z. Changyu, P. Jian, L. Jian, and H. Xiaohua, "Creep Behavior of CP-Ti TA2 at Low Temperature and Intermediate Temperature," *Rare Metal Materials and Engineering*, vol. 46, pp. 1463-1468, 2017/06/01/ 2017.
- [96]. Y. Gao, *Surface modification of TA2 pure titanium by low energy high current pulsed electron beam treatments* vol. 257, 2011.